Dual inhibition of cathepsin G and chymase reduces myocyte death and improves cardiac remodeling after myocardial ischemia reperfusion injury

Bahman Hooshdaran[1], **Mikhail A. Kolpakov**[1], **Xinji Guo**[1], **Sonni A. Miller**[1], **Tao Wang**[1], **Douglas G. Tilley**[2], **Khadija Rafiq**[3], and **Abdelkarim Sabri**[1]

[1]Cardiovascular Research Center, Lewis Katz School of Medicine, Temple University, MERB 1045, 3500 N. Broad Street, Philadelphia, PA 19140, USA

[2]Center of Translational Medicine, Lewis Katz School of Medicine, Temple University, Philadelphia, PA, USA

[3]Center of Translational Medicine, Thomas Jefferson University, Philadelphia, PA, USA

Abstract

Early reperfusion of ischemic cardiac tissue increases inflammatory cell infiltration which contributes to cardiomyocyte death and loss of cardiac function, referred to as ischemia/reperfusion (IR) injury. Neutrophil- and mast cell-derived proteases, cathepsin G (Cat.G) and chymase, are released early after IR, but their function is complicated by potentially redundant actions and targets. This study investigated whether a dual inhibition of Cat.G and chymase influences cardiomyocyte injury and wound healing after experimental IR in mice. Treatment with a dual Cat.G and chymase inhibitor (DCCI) immediately after reperfusion blocked cardiac Cat.G and chymase activity induced after IR, which resulted in decreased immune response in the infarcted heart. Mice treated with DCCI had less myocardial collagen deposition and showed preserved ventricular function at 1 and 7 days post-IR compared with vehicle-treated mice. DCCI treatment also significantly attenuated focal adhesion (FA) complex disruption and myocyte degeneration after IR. Treatment of isolated cardiomyocytes with Cat.G or chymase significantly promoted FA signaling downregulation, myofibril degeneration and myocyte apoptosis. Conversely, treatment of cardiac fibroblasts with Cat.G or chymase induced FA signaling activation and increased their migration and differentiation to myofibroblasts. These opposite responses in cardiomyocytes and fibroblasts were blocked by treatment with DCCI. These findings show that Cat.G and chymase are key mediators of myocyte apoptosis and fibroblast migration and differentiation that play a role in adverse cardiac remodeling and function post-IR. Thus, dual targeting of neutrophil- and mast cell-derived proteases could be used as a novel therapeutic strategy to reduce post-IR inflammation and improve cardiac remodeling.

Abdelkarim Sabri sabri@temple.edu.

Keywords

Myocardial ischemia–reperfusion; Inflammatory serine proteases; Cardioprotection; Inflammation

Introduction

Restoration of blood flow after acute myocardial infarction limits infarct size and reduces mortality. However reestablishing blood flow is often followed by a second set of stresses, a phenomenon referred to as ischemia–reperfusion (IR) injury, which can result in additional myocardial damage and account for up to half of total infarct size[8, 9, 39]. The factors contributing to IR injury are complex and include microvascular obstruction, inflammation, release of reactive oxygen species, myocardial stunning, and activation of cardiac cells apoptosis and necrosis [8, 39, 42]. A large amount of the early cardiac tissue damage that occurs during inflammation post-IR is mediated through early activation of neutrophils and mast cells, which produce reactive oxygen radicals and release granules containing proteolytic enzymes that are chemoattractants for other leukocyte populations [4, 15, 19]. While extensive research has explored the mechanisms responsible for the activation of inflammatory-derived cytokines/chemokines and reactive oxygen species and their roles in the infarcted heart, there is a paucity of information regarding the role of neutrophil- and mast cell-derived serine proteases on cardiac injury post-IR [10].

Inflammatory serine proteases (ISPs) derived from neutrophils, such as cathepsin G (Cat.G), elastase, and proteinase 3, and from mast cells, such as chymase and tryptase, are enzymes known mainly for their function in the intracellular killing of pathogens [2, 24]. Their extra-cellular release upon leukocyte activation is traditionally regarded as the primary reason for tissue damage at the sites of inflammation. However, some evidence indicates that ISPs may also be key regulators of the inflammatory response [2, 24]. ISPs cleave and functionally modulate a number of protein substrates, including clotting factors, neutrophil chemoattractants, and extracellular (ECM) components (e.g., proteoglycans, collagen, elastin, fibronectin) [35, 40]. The adverse effects of Cat.G and chymase go beyond the breakdown of matrix proteins or the generation of cytokines and chemokines, which stimulate the infiltration of inflammatory cells. Recent studies from our lab and others identified cardiac myocytes and fibroblasts as additional cell targets for Cat.G and chymase [30, 32, 33]. Both Cat.G and chymase induce morphological changes in cardiomyocytes that disrupt intercellular contacts and focal adhesion (FA) signaling [13, 30]. Chymase can also trigger signaling in cardiac fibroblasts that leads either to proliferation at low dose or death by autophagy at high dose [5, 7]. However, the molecular mechanisms by which Cat.G and chymase modulate cardiac myocyte and fibroblast function are still largely unknown.

Because human Cat.G and chymase have similar active sites and share some common functions [35, 40], assessing their function in human diseases is complicated by potentially redundant functions and targets. One strategy has been to develop dual Cat.G-chymase inhibitors (DCCI) [6]. The DCCI used in this study was shown to selectively inhibit Cat.G and chymase in vitro, with little effect on several other serine proteases such as thrombin, factor Xa, trypsin, tryptase, proteinase 3, and elastase [6]. DCCI has been shown to

markedly reduce neutrophil influx and nitric oxide levels associated with lipopolysaccharide-induced lung inflammation [23]. In the present study, we describe how DCCI administration to mice subjected to IR injury resulted in reduced myocardial Cat.G and chymase activity and pathologic remodeling associated with IR. We show that it also reduced collagen deposition within the myocardium and prevented left ventricular (LV) dysfunction. Our findings provide evidence that a dual inhibitor targeting Cat.G and chymase may be of therapeutic benefit in protecting the heart from IR injury.

Methods

Experimental protocol

All mice were maintained in accordance with protocols approved by the Animal Care and Use Committee of Temple University. Ten week-old C57BL6 male mice were anesthetized with a mixture of ketamine (100 mg/kg) and xylazine (10 mg/kg) and left thoracotomy was performed under mechanical ventilation. Body temperature was maintained by a heated surgical platform and was monitored throughout surgery using a rectal sensor. A 6-0 suture with a slipknot was tied around the left anterior descending (LAD) coronary artery to produce ischemia. Consistent elevation of the ST segment was observed in lead II tracings following occlusion of the LAD coronary vessel. Regional ischemia was confirmed by visual inspection under a dissecting microscope (Nikon) by discoloration of the occluded distal myocardium. The ligation was released after 30 min of ischemia and the tissue was allowed to reperfuse as confirmed by visual inspection. The chest wall was closed with 8-0 silk and then the animal was removed from the ventilator and kept warm in the cage maintained at 37 °C overnight. A sham procedure constituted the surgical incision without LAD ligation. Hearts were harvested after 1 or 7 days of reperfusion.

To investigate the role of Cat.G and chymase, mice were randomly divided into 4 major groups, consisting of: (1) sham mice receiving DCCI (EMD Millipore, 219372) (10 mg/kg body weight; $n = 8$); (2) sham mice receiving vehicle (0.1% DMSO in NaCl 0.9%; $n = 8$); (3) IR mice receiving 10 mg/kg DCCI ($n = 8$); and (4) IR mice receiving vehicle (0.1% DMSO in NaCl 0.9%, $n = 8$). DCCI or its vehicle was administered by means of single intravenous bolus injection immediately after reperfusion of the ischemic myocardium (for mice subjected to IR for 24 h) and treated daily via intraperitoneal injection (for mice subjected to IR injury for 7 days).

Data analysis

All results are reported as mean ± SEM. Comparison of two groups was accomplished using an unpaired Student's *t* test. One-way ANOVA followed by the Tukey post hoc test was used to compare multiple groups; two-way ANOVA and subsequent Tukey test were performed to compare groups with different time points. $P < 0.05$ was considered to be statistically significant. All in vitro experiments were performed at least three times from three different cultures and the data values were scaled to controls. A value of $P < 0.05$ was considered statistically significant.

An expanded methods section is provided in the Supplemental material.

Results

DCCl treatment attenuates the severity of the acute inflammatory response after IR

Initially, we determined the time course of the increase in myocardial neutrophil and mast cell-derived protease activity at 3 h, 6 h, 1 day and 7 days after IR. Cat.G and elastase protease activity underwent early transient increases, returning to baseline at 7 days post-IR (Fig. 1a, b), while chymase activity increased early and was sustained for over 7 days post-IR (Fig. 1c). Immunohistochemistry results further corroborate the changes observed in protease activity, as Cat.G-positive cells in the heart were markedly increased at 1 day post-IR, but decreased to baseline at 7 days post-IR (Fig. 1d, e). In contrast, chymase-positive cells were elevated at both 1 and 7 days post-IR (Fig. 1d, f). These data highlight the differential kinetics of Cat.G and chymase activity following acute cardiac injury, and suggest that targeting both could have more impact on preventing the deleterious effects of sustained protease activity over time.

To evaluate the efficacy of inhibiting both Cat.G and chymase in preventing the sequelae of IR injury, we treated mice with DCCl for 1 and 7 days. DCCl was given during reperfusion at 10 mg/kg intravenously and thereafter injected every day intraperitoneally for 6 days. This dose was based on the biological half-life of DCCl and on in vivo experiments in which the compound's effectiveness was evaluated in an acute lung injury model [23]. The mice were killed at 1 day after IR (a time point coinciding with peak inflammatory cell infiltration and myocyte loss) and at 7 days post-IR, coinciding with peak scar formation and repair [4]. At 1 and 7 days post-IR, myocardial Cat.G and chymase proteolytic activity were significantly reduced in DCCl-treated mice compared with vehicle-treated mice (Fig. 2a, b), while Cat.G and chymase activity were not significantly altered in DCCl- and vehicle-treated sham-operated mice. Myocardial myeloperoxidase (MPO) activity was measured to determine the impact of DCCl on the infiltration of inflammatory cells after IR. In DCCl-treated mice, MPO activity was markedly reduced compared with that in vehicle-treated mice (Fig. 2c). Post-IR immunohistological examination of DCCl- and vehicle treated mouse hearts further corroborated these data (Fig. 2d), as the number of MPO-positive neutrophils was markedly reduced in the infarcted regions of DCCl-versus vehicle-treated mouse hearts (Fig. 2d, e). DCCl-treated mice also show less infiltration of mast cells (Fig. 2d, f), Mac-3-positive macrophages and CD3-positive T-cells (Supplemental Fig. S1) in the infarcted area compared to vehicle-treated group. Moreover, activation of pro-inflammatory signaling pathways, STAT3 and NF-kB, and accumulation of pro-inflammatory cytokines that mediate early infiltration of leukocytes in the infarcted myocardium, tumor necrosis factor (TNF)-α and interleukin (IL)-1β [12, 18], were markedly reduced in the infarcted regions of DCCl-versus vehicle-treated mouse hearts (Fig. 2g). Collectively, these data show that dual inhibition of Cat.G and chymase activity reduces early inflammatory responses following IR injury.

Dual inhibition of Cat.G and chymase improves cardiac function

We next explored the impact of Cat.G and chymase inhibition on cardiac function at 1 and 7 days post-IR. DCCl treatment did not alter baseline heart weight-to-body weight ratio, heart rate, or LV dilatation in sham-operated animals (Fig. 3; Supplemental Tables 1, 2). However,

DCCI-treated mice displayed a significant preservation in post-IR cardiac function versus vehicle-treated mice, including LV ejection fraction and fractional shortening (Fig. 3a, b). LV end-systolic and diastolic dimensions (Fig. 3c, d) were also shown to undergo better preservation post-IR in DCCI-versus vehicle-treated mice. Morphometric analysis indicates the presence of cardiac hypertrophy and concomitant signs of cardiac failure, such as an increase in lung weight, in vehicle-treated mice, whereas only the latter pathological response was reduced in the DCCI-treated mice at 7 days post-IR (Fig. 3e, f; Supplemental Table 2). Infarct size measurements as percentage of area at risk or LV circumference indicated $34 \pm 2\%$ and $38 \pm 4\%$ of the LV to be affected by the infarct at 1 and 7 days in vehicle-treated mice, respectively, whereas the infarct accounted for $24 \pm 3\%$ and $26 \pm 2\%$ of the LV in DCCI-treated mice (Fig. 3g, h). Thus, the integrity of the infarcted area was maintained after IR in DCCI-treated mice with reduced LV dilatation compared to vehicle-treated mice, which results in a better cardiac function post-IR.

Dual inhibition of Cat.G and chymase is cardioprotective

The extent of myocardial infarct and impairment in cardiac performance depends on the levels of cardiomyocyte loss post-IR, which we measured in vehicle- and DCCI-treated mice 1 day post-IR via terminal deoxynucleotidyl transferase dUTP nick end labeling (TUNEL). Consistent with a protective effect of protease inhibition at time of IR, mice that were treated with DCCI had a reduced number of TUNEL-positive myocytes 1 day following reperfusion compared to vehicle-treated mice (Fig. 4a, c). Cardiac caspase-3 activity (Fig. 4d) and circulating plasma levels of cardiac troponin-I (cTnI, Fig. 4e) were also reduced in DCCI-versus vehicle-treated mice 1 day post-IR. DCCI-treated mice also showed reduced expression of pro-apoptotic molecule Bax and enhanced accumulation of signaling molecules known to inhibit cell apoptosis such as XIAP compared to vehicle-treated mice (Fig. 4f), confirming the cytoprotective effect of dual inhibition of Cat.G and chymase at the time of injury.

DCCI protects impaired FA signaling induced after IR

Both Cat.G and chymase have been shown to induce myocyte apoptosis via downregulation of FA signaling in vitro [30, 32]. Thus, we explored whether DCCI treatment alters IR-induced FA signaling in the heart. Vehicle-treated mice showed decreased FAK and paxillin protein accumulation that correlated with a decrease in cTnI expression (Fig. 4g). In contrast, DCCI-treated mice showed less IR-induced FAK, paxillin and cTnI degradation compared to vehicle-treated mice. Collectively, these data show that dual Cat.G and chymase inhibition protects FA signaling and induces cardioprotective signaling events to promote myocyte survival in the heart following IR.

To determine whether FA signaling downregulation results from degradation of ECM proteins, we performed experiments to determine the impact of DCCI on fibronectin (Fn) expression post-IR (Supplemental Fig. S2). Results show a slight increase in Fn accumulation at ~220 kD at 1 day post-IR in vehicle-treated mice. However, we cannot specify whether the source of Fn is from plasma-derived soluble Fn or from intra-cardiac secreted cellular Fn. Basal Fn accumulation was increased in shams treated with DCCI, but

its level remained similar in DCCI-treated IR mice. These data suggest that Fn degradation does not account for the impaired FA signaling observed after IR.

To directly demonstrate that the cardioprotective effects of DCCI after IR may result from direct actions of Cat.G and chymase on cardiomyocytes, we investigated the effect of DCCI on cardiomyocyte apoptosis induced by these proteases. Treatment of neonatal rat cardiomyocytes (NRCMs) with Cat.G or chymase for 8 h markedly induced myocyte detachment and increased caspase-3 activity (Fig. 5a, b). In contrast, treatment with DCCI blunted both myocyte detachment and cell death induced by Cat.G and chymase treatment. Conversely, treatment of neonatal rat cardiac fibroblasts (NRCFs) with Cat.G or chymase for 8 h did not induce detachment or caspase-3 activity (Fig. 5a, c), demonstrating a differential response between myocytes and fibroblasts after Cat.G or chymase treatment.

To delineate the mechanisms involved in the differential response between cardiac myocytes and fibroblasts, we assessed the impact of DCCI on Cat.G- and chymase-induced FA signaling, which we have shown previously to play an important role in Cat.G- and chymase-induced myocyte detachment and apoptosis [30, 32]. Myocytes treated with Cat.G or chymase showed markedly reduced FAK and paxillin tyrosine phosphorylation after treatment for 10 min (Fig. 5d), which were markedly reduced by DCCI. DCCI treatment also inhibited FAK, paxillin and cTnI degradation induced by Cat.G treatment for 4 h (Supplemental Fig. S3). Conversely, Cat.G or chymase treatment induced FAK and paxillin tyrosine phosphorylation in fibroblasts, demonstrating activation of FA signaling (Fig. 5e). These data highlight a major molecular mechanism by which Cat.G and chymase signaling induces distinct outcomes in cardiomyocytes versus fibroblasts.

Mice treated with DCCI are protected against profibrotic remodeling induced after IR injury

Based on our findings that Cat.G and chymase do not induce fibroblast detachment and death, we next explored the potential role of DCCI on cardiac fibrosis and remodeling responses post-IR. Collagen fractional area in the non-infarcted region of the heart was not different between DCCI- and vehicle-treated groups (Fig. 6a, b). However, DCCI-treated mice had significantly less collagen accumulation in the infarcted region compared with vehicle-treated mice at day 7 post-IR. To determine the mechanisms of decreased collagen accumulation after DCCI treatment, we evaluated accumulation of myofibroblasts, which are a primary source of extracellular matrix (ECM) protein synthesis in the infarcted myocardium [38]. Analysis of smooth muscle α-actin (SMA) staining showed minimal accumulation of myofibroblasts in sham-operated hearts (not shown) which progressively increased in vehicle-treated mice infarcts (Fig. 6a, c). DCCI-treated mice showed reduced myofibroblast density and decreased accumulation of profibrotic CTGF and TGF-β gene expression in the infarcted heart (Fig. 6c, d). We also investigated whether DCCI treatment affects ECM degradation after IR. Both pro- and active-MMP2/9 levels, as well as gelatinase activity, were significantly reduced in the infarcts of DCCI-versus vehicle-treated mice 7 days post-IR (Fig. 6e, f). Levels of pro-MMP2/9 were similar in DCCI-treated shams compared to vehicle-treated mice. Thus, inhibition of Cat.G and chymase activity results in fibroblast differentiation and activity following IR that is associated with diminished ECM accumulation and preserved cardiac contractile dysfunction.

Cat.G and chymase induce fibroblast migration and differentiation

Because fibroblasts are important components of fibrosis, we determined whether Cat.G or chymase directly influenced fibroblast migration and ECM protein accumulation in isolated neonatal rat cardiac fibroblasts. In control experiments, we established that treatment with Cat.G or chymase increased SM α-actin expression, indicating fibroblast differentiation to myofibroblasts (Fig. 7a). Similar differentiation to myofibroblasts was also observed in adult mouse cardiac fibroblasts treated with Cat.G or chymase after SM α-actin staining (Supplemental Fig. S4) Cat.G or chymase treatment also increased TGF-β1 and collagen I expression, indicative of enhanced secretory phenotype. Conversely, concurrent treatment with DCCI blocked Cat.G- or chymase-induced responses in cardiac fibroblasts.

We next determined whether Cat.G- or chymase-induced fibroblast differentiation modulates activation of NF-κB and STAT3 activation, important mediators of cardiac inflammation and fibrosis following injury [4]. Cat.G or chymase treatment was sufficient to activate endogenous NF-κB and STAT3, responses that were abolished by treatment with DCCI (Fig. 7b). The proinflammatory effect of Cat.G and chymase was further corroborated by changes in the expression of the NF-κB/STAT3-responsive genes such as TNF-α and IL-1β, which were upregulated in Cat.G- or chymase-treated fibroblasts compared with control cells, and treatment with DCCI blocked these responses (Fig. 7c).

Given these findings with respect to cell differentiation, we also sought to determine whether fibroblast migration and differentiation are sensitive to DCCI. Figure 7d shows representative phase-contrast micrographs of scratch assays of confluent fibroblast cell monolayers. Both Cat.G and chymase increased fibroblast migration compared with vehicle (Fig. 7e). Importantly, the degree of cell migration observed with Cat.G was not significantly different from that of chymase-treated cells. Fibroblast migration induced by Cat.G or chymase was significantly diminished after treatment with DCCI compared with vehicle-treated cultures. Collectively, these data demonstrate that Cat.G and chymase can directly trigger fibroblast migration and differentiation to myofibroblasts.

Discussion

The current study provides new insights into the mechanisms of pathological remodeling during early induction of IR injury. We demonstrate that dual inhibition of Cat.G and chymase activity was associated with a decrease in the pathologic severity of the cardiac inflammatory response, myocyte apoptosis and fibrosis post-IR. The reduced adverse remodeling in the DCCI-treated mice was associated with improved myocardial function when compared with that in the vehicle-treated mice. Interestingly, we found that Cat.G and chymase activated signaling pathways that culminated to detachment and apoptosis of myocytes, while they promoted migration and differentiation of fibroblasts. This dichotomous outcome between cardiac myocytes and fibroblasts was likely related to differential regulation of FA signaling by Cat.G and chymase. These novel findings show that one of the earliest events in mediating cardiac dysfunction after IR injury involves an increased activation of Cat.G and chymase and points to DCCI as a therapeutic benefit.

The major effect underlying the absence of severe tissue injury after cardiac IR in DCCI-treated mice is the inability to sustain the presence of inflammatory cells in the heart after reperfusion. The decreased Cat.G and chymase activity observed after reperfusion in ischemic hearts from DCCI-treated mice was accompanied by a decrease in infiltration of neutrophils and mast cells. These cells have been reported to infiltrate early after myocardial injury and produce chemokines, which may amplify and sustain the intensity of leukocyte migration to the site of myocardial injury [1, 34]. Accordingly, we show that DCCI-treated mice hearts have reduced production of inflammatory cytokines, IL-1β and TNF-α, and decreased accumulation of macrophages and T cells in the infarcted heart at day 1 and 7 post-IR compared to vehicle-treated mice. These data extend previous studies showing the role of Cat.G and chymase in mediating monocytes, neutrophils or T cells migration in vitro and in the processing and maturation of several cytokines and chemokines including IL-1α, IL-6, and TNF-α [24]. In addition to these direct actions of Cat.G and chymase on inflammatory cells, DCCI-treated mice also show limited tissue exposure to myeloperoxidase, which is a major mediator of tissue damage after injury through generation of hypochlorous acid and reactive oxygen species [27]. The short term of myeloperoxidase activity observed in the heart from DCCI-treated animals argues that the initial burst of myeloperoxidase does not induce or sustain substantial injury in the absence of Cat.G or chymase. Collectively, these data emphasize the importance of Cat.G and chymase in mediating early cardiac immune response post-IR.

The limited exposure of the ischemic heart to Cat.G- and chymase-mediated events during reperfusion in DCCI-treated mice resulted in clear reductions in tissue injury and improvement in cardiac contractile function. One important consequence was a substantial decrease in cardiomyocyte apoptosis in the ischemic hearts. Several studies have demonstrated cardiomyocyte apoptosis after reperfusion of ischemic hearts and the correlation between the number of apoptotic cells and the severity of cardiac dysfunction [17]. Whether the absence of Cat.G/chymase or the resultant limited exposure to myeloperoxidase or other inflammatory cell-derived cytokines/chemokines underlie this decrease in apoptosis cannot be defined from this study. However, both Cat.G and chymase have been shown to act directly on cardiomyocytes and promote apoptosis [30, 32]. In this study, we found that treatment with DCCI prevented FA protein degradation, myofibril degeneration and myocyte apoptosis induced after 24 h of IR injury and after treatment of isolated cardiomyocytes with Cat.G or chymase. The fact that the kinetics of FA signaling downregulation coincide with myocyte apoptosis post-IR strongly suggests that one of the earliest events leading to myocyte apoptosis after IR injury may involve a loss of ECM network surrounding myocytes and a lack of survival signaling emanating from ECM receptors, integrins, in response to elevated levels of Cat.G and chymase. The suppression of FA signaling downregulation by DCCI further supports the active role of Cat.G and chymase on cardiomyocyte stress during acute IR.

The induction of myocyte death has been proposed to be a principal factor leading to the tissue fibrosis that develops after IR injury [22]. Consistent with the lack of sustained Cat.G/chymase activity and decreased apoptosis of myocytes, there was a clear decrease in collagen deposition observed in hearts from DCCI-treated mice post-IR when compared with vehicle-treated mice. We also found that DCCI-treated mice present less myofibroblast

accumulation at day 7 post-IR. This latter has been shown to be a primary source of ECM protein synthesis and pro-inflammatory cytokines in the infarcted myocardium [38]. Moreover, DCCI may have more direct antifibrotic effects as Cat.G and chymase may liberate TGF-β from the ECM, thereby stimulating fibroblast differentiation and ECM synthesis [21, 26, 41, 43]. In this study, we show that DCCI treatment blocked both TGF-β and CTGF accumulation in the infarcted heart at day 7 post-IR and in isolated fibroblasts treated with Cat.G or chymase, which resulted in a decrease in ECM accumulation, fibroblast migration and differentiation to myofibroblasts. Cat.G and chymase can also affect ECM accumulation through activation of MMP-2 and −9 [31, 36] which could degrade cardiac interstitial matrix, expand the healing infarct [25] and promote cardiac dilatation [3]. We show that DCCI treatment attenuated MMP-2/9 activation after IR in vivo and in isolated cardiac fibroblasts exposed to Cat.G or chymase (Supplemental Fig. S5), suggesting that Cat.G and chymase-dependent activation of MMPs is also important in post-IR infarct remodeling and function.

The pleiotropic effects of Cat.G and chymase on cardiac myocytes and fibroblasts raise the intriguing question about the mechanisms by which these extracellular proteases initiate their effects in both cells. We have previously documented the role of MMP activation as a mechanism by which Cat.G induces FA signaling downregulation and myocyte apoptosis [31]. Consistent with these findings, DCCI treatment inhibited Cat.G- and chymase-induced MMP2 activation and FA protein degradation in cardiomyocytes (Supplemental Fig. S5). Interestingly, in contrast to cardiomyocytes, Cat.G and chymase led to FA signaling activation in fibroblasts that culminated to fibroblast migration and differentiation. These data, although are in line with the role of FAK activation in mediating cell survival and growth, suggest a different mechanism of FA signaling regulation between myocytes and fibroblasts. Previous studies from our group in myocytes showed the role of protein tyrosine phosphatase SHP2 in mediating Cat.G-induced FA signaling downregulation and myocyte apoptosis [31, 32]. Whether SHP2 activation is differentially regulated in cardiac fibroblasts versus cardiomyocytes in response to Cat.G or chymase needs further investigation. These data collectively show the pleiotropic actions of these proteases to trigger cardiomyocyte death and fibroblast migration/differentiation and the beneficial effect of DCCI treatment in preventing these effects.

The current study provides evidence that targeting neutrophil- and mast cell-derived proteases was efficient in protecting the heart from early myocyte death and excessive fibroblast migration and ECM accumulation that contribute to adverse cardiac remodeling and contractile dysfunction (Supplemental Fig. S6). Moreover, DCCI can modulate cardiac remodeling and function indirectly by inhibiting Cat.G and chymase actions to convert angiotensin I to angiotensin II [20, 28], a known humoral factor that promotes cardiac hypertrophy, fibrosis, and remodeling [37]. Based on evidence that Cat.G and chymase have similar active sites, share some common targets and have potentially redundant functions, our strategy has been to use a dual inhibitor that selectively targets both Cat.G and chymase, without affecting other serine proteases [6]. There has been considerable interest to develop inhibitors of neutrophil- and mast cell-derived proteases, which contribute to cardiac injury and inflammation. Previous studies have shown the beneficial effect of inhibiting chymase on IR injury in dogs and pigs [29, 44]. However, in these studies there was no assessment of

chymase inhibition on a more prolonged reperfusion on myocardial function and infarct extension. In rodents, the use of chymase inhibitor monotherapy provided mixed results with studies showing improved survival and reduced post-my-ocardial infarction cardiac hypertrophy and dysfunction with chymase inhibitor monotherapy [14, 16], while others were negative [11]. This discrepancy using chymase inhibitor monotherapy could be related to the fact that other inflammatory proteases such as Cat.G may play a redundant role in the pathophysiology of IR injury. Therefore, our results with DCCI suggest that inhibition of more than one crucial inflammatory protease might afford effective pharmacotherapy and show that restoration of a "protease–antiprotease balance" by the administration of exogenous inhibitors reduces excessive accumulation of inflammatory cells and their secreted proteases and could have therapeutic utility after myocardial IR injury.

In conclusion, a dual inhibitor targeting Cat.G and chymase is effective in reducing the pathologic severity related to IR injury in association with its ability to limit myocardial proteolytic activity. By attenuating collagen deposition within the myocardium and improving LV function, DCCI may ultimately decrease the progression to heart failure. Our study has, therefore, provided important data to support a previously unknown mechanism implicating Cat.G and chymase in the progression of this disease and the theoretical benefit of using a dual inhibitor targeting Cat.G and chymase in the therapy of acute IR injury.

Supplementary Material

Refer to Web version on PubMed Central for supplementary material.

Acknowledgements

References

1. Beghdadi W, Madjene LC, Benhamou M, Charles N, Gautier G, Launay P, Blank U (2011) Mast cells as cellular sensors in inflammation and immunity. Front Immunol 2:37. doi:10.3389/fimmu. 2011.00037 [PubMed: 22566827]

2. Caughey GH (2016) Mast cell proteases as pharmacological targets. Eur J Pharmacol 778:44–55. doi:10.1016/j.ejphar.2015.04.045 [PubMed: 25958181]

3. Ducharme A, Frantz S, Aikawa M, Rabkin E, Lindsey M, Rohde LE, Schoen FJ, Kelly RA, Werb Z, Libby P, Lee RT (2000) Targeted deletion of matrix metalloproteinase-9 attenuates left ventricular enlargement and collagen accumulation after experimental myocardial infarction. J Clin Investig 106:55–62. doi:10.1172/JCI8768 [PubMed: 10880048]

4. Frangogiannis NG (2012) Regulation of the inflammatory response in cardiac repair. Circ Res 110:159–173. doi:10.1161/CIRCRESAHA.111.243162 [PubMed: 22223212]

5. Fu L, Wei C-C, Powell PC, Bradley WE, Ahmad S, Ferrario CM, Collawn JF, Dell'Italia LJ (2016) Increased fibroblast chymase production mediates procollagen autophagic digestion in volume overload. J Mol Cell Cardiol 92:1–9. doi:10.1016/j.yjmcc.2016.01.019 [PubMed: 26807691]

6. Greco MN, Hawkins MJ, Powell ET, Almond HR, Corcoran TW, de Garavilla L, Kauffman JA, Recacha R, Chattopadhyay D, Andrade-Gordon P, Maryanoff BE (2002) Nonpeptide inhibitors of cathepsin G: optimization of a novel β-ketophosphonic acid lead by structure-based drug design. J Am Chem Soc 124:3810–3811. doi:10.1021/ja017506h [PubMed: 11942800]

7. Hara M, Matsumori A, Ono K, Kido H, Hwang M-W, Miyamoto T, Iwasaki A, Okada M, Nakatani K, Sasayama S (1999) Mast cells cause apoptosis of cardiomyocytes and proliferation of other intramyocardial cells in vitro. Circulation 100:1443–1449. doi:10.1161/01.cir.100.13.1443 [PubMed: 10500047]

8. Heusch G, Gersh BJ (2017) The pathophysiology of acute myocardial infarction and strategies of protection beyond reperfusion: a continual challenge. Eur Heart J 38:774–784. doi:10.1093/eurheartj/ehw224 [PubMed: 27354052]

9. Heusch G, Libby P, Gersh B, Yellon D, Bohm M, Lopaschuk G, Opie L (2014) Cardiovascular remodelling in coronary artery disease and heart failure. Lancet (London, England) 383:1933–1943. doi:10.1016/s0140-6736(14)60107-0

10. Heutinck K, ten Berge I, Hack C, Hamann J, Rowshani A (2010) Serine proteases of the human immune system in health and disease. Mol Immunol 47:1943–1955 [PubMed: 20537709]

11. Hoshino F, Urata H, Inoue Y, Saito Y, Yahiro E, Ideishi M, Arakawa K, Saku K (2003) Chymase inhibitor improves survival in hamsters with myocardial infarction. J Cardiovasc Pharmacol 41:S11–S18 (**ISSN print: 0160-2446, accession: 00005344-200301001-00004**) [PubMed: 12688390] **ISSN print: 0160-2446, accession: 00005344-200301001-00004)**

12. Hwang M-W, Matsumori A, Furukawa Y, Ono K, Okada M, Iwasaki A, Hara M, Miyamoto T, Touma M, Sasayama S (2001) Neutralization of interleukin-1b in the acute phase of myocardial infarction promotes the progression of left ventricular remodeling. J Am Coll Cardiol 38:1546–1553. doi:10.1016/S0735-1097(01)01591-1 [PubMed: 11691538]

13. Iacoviello L, Kolpakov V, Salvatore L, Amore C, Pintucci G, de Gaetano G, Donati MB (1995) Human endothelial cell damage by neutrophil-derived cathepsin G. Role of cytoskeleton rearrangement and matrix-bound plasminogen activator inhibitor-1. Arterioscler Thromb Vasc Biol 15:2037–2046. doi:10.1161/01.ATV.15.11.2037 [PubMed: 7583587]

14. Jin D, Takai S, Yamada M, Sakaguchi M, Kamoshita K, Ishida K, Sukenaga Y, Miyazaki M (2003) Impact of chymase inhibitor on cardiac function and survival after myocardial infarction. Cardiovasc Res 60:413–420. doi:10.1016/S0008-6363(03)00535-2 [PubMed: 14613871]

15. Kain V, Prabhu SD, Halade GV (2014) Inflammation revisited: inflammation versus resolution of inflammation following myocardial infarction. Basic Res Cardiol 109:444. doi:10.1007/s00395-014-0444-7 [PubMed: 25248433]

16. Kanemitsu H, Takai S, Tsuneyoshi H, Nishina T, Yoshikawa K, Miyazaki M, Ikeda T, Komeda M (2006) Chymase inhibition prevents cardiac fibrosis and dysfunction after myocardial infarction in rats. Hypertens Res 29:57–64. doi:10.1291/hypres.29.57 [PubMed: 16715654]

17. Krijnen PAJ, Nijmeijer R, Meijer CJLM, Visser CA, Hack CE, Niessen HWM (2002) Apoptosis in myocardial ischaemia and infarction. J Clin Pathol 55:801–811. doi:10.1136/jcp.55.11.801 [PubMed: 12401816]

18. Kukielka GL, Smith CW, Manning AM, Youker KA, Michael LH, Entman ML (1995) Induction of interleukin-6 synthesis in the myocardium: potential role in postreperfusion inflammatory injury. Circulation 92:1866–1875. doi:10.1161/01.CIR.92.7.1866 [PubMed: 7671371]

19. Levick SP, Meléndez GC, Plante E, McLarty JL, Brower GL, Janicki JS (2011) Cardiac mast cells: the centrepiece in adverse myocardial remodelling. Cardiovasc Res 89:12–19. doi:10.1093/cvr/cvq272 [PubMed: 20736239]

20. Lindberg BF, Gyllstedt E, Andersson K-E (1997) Conversion of angiotensin I to angiotensin II by chymase activity in human pulmonary membranes. Peptides 18:847–853. doi:10.1016/S0196-9781(97)00011-9 [PubMed: 9285934]

21. Lindstedt KA, Wang Y, Shiota N, Saatinen J, Hyytiainen M, Kokkonen JO, Keski-Oja J, Kovanen PT (2001) Activation of paracrine TGF-β1 signaling upon stimulation and degranulation of rat serosal mast cells: a novel function for chymase. FASEB J 15:1377–1388. doi:10.1096/fj.00-0273com [PubMed: 11387235]

22. Mani K (2008) Programmed cell death in cardiac myocytes: strategies to maximize post-ischemic salvage. Heart Fail Rev 13(2):193–209. doi:10.1007/s10741-007-9073-7 [PubMed: 18176842]

23. Maryanoff BE, Garavilla Ld, Greco MN, Haertlein BJ, Wells GI, Andrade-Gordon P, Abraham WM (2010) Dual inhibition of cathepsin G and chymase is effective in animal models of

pulmonary inflammation. Am J Resp Crit Care Med 181:247–253. doi:10.1164/rccm. 200904-0627OC [PubMed: 19875688]

24. Meyer-Hoffert U, Wiedow O (2011) Neutrophil serine proteases: mediators of innate immune responses. Curr Opin Hematol 18:19–24. doi:10.1097/MOH.0b013e32834115d1 [PubMed: 21042214]

25. Mukherjee R, Brinsa TA, Dowdy KB, Scott AA, Baskin JM, Deschamps AM, Lowry AS, Escobar GP, Lucas DG, Yarbrough WM, Zile MR, Spinale FG (2003) Myocardial infarct expansion and matrix metalloproteinase inhibition. Circulation 107:618–625. doi:10.1161/01.cir. 0000046449.36178.00 [PubMed: 12566376]

26. Murphy E, Steenbergen C (2008) Mechanisms underlying acute protection from cardiac ischemia-reperfusion injury. Physiol Rev 88:581–609. doi:10.1152/physrev.00024.2007 [PubMed: 18391174]

27. Nicholls SJ, Hazen SL (2005) Myeloperoxidase and cardiovascular disease. Arter Thromb Vasc Biol 25:1102–1111. doi:10.1161/01.ATV.0000163262.83456.6d

28. Owen CA, Campbell EJ (1998) Angiotensin II generation at the cell Surface of activated neutrophils: novel cathepsin G-mediated catalytic activity that is resistant to inhibition. J Immunol 160:1436–1443 **(print ISSN: 0022-1767, online ISSN: 1550-6606)** [PubMed: 9570564] **(print ISSN: 0022-1767, online ISSN: 1550-6606)**

29. Oyamada S, Bianchi C, Takai S, Chu LM, Sellke FW (2011) Chymase inhibition reduces infarction and matrix metalloproteinase-9 activation and attenuates inflammation and fibrosis after acute myocardial ischemia/reperfusion. J Pharmacol Exp Ther 339:143–151. doi:10.1124/jpet. 111.179697 [PubMed: 21795433]

30. Pat B, Chen Y, Killingsworth C, Gladden JD, Shi K, Zheng J, Powell PC, Walcott G, Ahmed MI, Gupta H, Desai R, Wei C-C, Hase N, Kobayashi T, Sabri A, Granzier H, Denney T, Tillson M, Dillon AR, Husain A, Dell'Italia LJ (2010) Chymase inhibition prevents fibronectin and myofibrillar loss and improves cardiomyocyte function and LV torsion angle in dogs with isolated mitral regurgitation. Circulation 122:1488–1495. doi:10.1161/circulationaha.109.921619 [PubMed: 20876440]

31. Rafiq K, Hanscom M, Valerie K, Steinberg S, Sabri A (2008) Novel mode for neutrophil protease cathepsin G-mediated signaling: membrane shedding of epidermal growth factor is required for cardiomyocyte anoikis. Circ Res 102:32–41. doi:10.1161/CIRCRESAHA.107.150573 [PubMed: 17975113]

32. Rafiq K, Kolpakov MA, Abdelfettah M, Streblow DN, Hassid A, Dell'Italia LJ, Sabri A (2006) Role of protein-tyrosine phosphatase SHP2 in focal adhesion kinase down-regulation during neutrophil cathepsin G-induced cardiomyocytes anoikis. J Biol Chem 281:19781–19792. doi: 10.1074/jbc.M513040200 [PubMed: 16690621]

33. Sabri A, Alcott SG, Elouardighi H, Pak E, Derian C, Andrade-Gordon P, Kinnally K, Steinberg SF (2003) Neutrophil cathepsin G promotes detachment-induced cardiomyocyte apoptosis via a protease-activated receptor-independent mechanism. J Biol Chem 278:23944–23954. doi:10.1074/ jbc.M302718200 [PubMed: 12707281]

34. Scapini P, Lapinet-Vera JA, Gasperini S, Calzetti F, Bazzoni F, Cassatella MA (2000) The neutrophil as a cellular source of chemokines. Immunol Rev 177:195–203. doi:10.1034/j. 1600-065X.2000.17706.x [PubMed: 11138776]

35. Sharony R, Yu P-J, Park J, Galloway A, Mignatti P, Pintucci G (2010) Protein targets of inflammatory serine proteases and cardiovascular disease. J Inflamm 7:45. doi: 10.1186/1476-9255-7-45

36. Tchougounova E, Lundequist A, Fajardo I, Winberg J-O, Å brink M, Pejler G (2005) A key role for mast cell chymase in the activation of pro-matrix metalloprotease-9 and pro-matrix metalloprotease-2. J Biol Chem 280:9291–9296. doi:10.1074/jbc.M410396200 [PubMed: 15615702]

37. Travers JG, Kamal FA, Robbins J, Yutzey KE, Blaxall BC (2016) Cardiac fibrosis: the fibroblast awakens. Circ Res 118:1021–1040. doi:10.1161/circresaha.115.306565 [PubMed: 26987915]

38. van den Borne SWM, Diez J, Blankesteijn WM, Verjans J, Hofstra L, Narula J (2010) Myocardial remodeling after infarction: the role of myofibroblasts. Nat Rev Cardiol 7:30–37. doi:10.1038/ nrcardio.2009.199 [PubMed: 19949426]

39. Vander Heide RS, Steenbergen C (2013) Cardioprotection and myocardial reperfusion: pitfalls to clinical application. Circ Res 113:464–477. doi:10.1161/circresaha.113.300765 [PubMed: 23908333]

40. Wiedow O, Meyer-Hoffert U (2005) Neutrophil serine proteases: potential key regulators of cell signalling during inflammation. J Intern Med 257:319–328. doi:10.1111/j. 1365-2796.2005.01476.x [PubMed: 15788001]

41. Wilson TJ, Nannuru KC, Singh RK (2009) Cathepsin G-mediated activation of pro-matrix metalloproteinase 9 at the tumor-bone interface promotes transforming growth factor-β signaling and bone destruction. Mol Cancer Res 7:1224–1233. doi:10.1158/1541-7786.mcr-09-0028 [PubMed: 19671689]

42. Yellon DM, Hausenloy DJ (2007) Myocardial reperfusion injury. N Engl J Med 357:1121–1135. doi:10.1056/NEJMra071667 [PubMed: 17855673]

43. Zhao X-Y, Zhao L-Y, Zheng Q-S, Su J-L, Guan H, Shang F-J, Niu X-L, He Y-P, Lu X-L (2008) Chymase induces profibrotic response via transforming growth factor-β1/Smad activation in rat cardiac fibroblasts. Mol Cell Biochem 310:159–166. doi:10.1007/s11010-007-9676-2 [PubMed: 18057996]

44. Zheng J, Wei C-C, Hase N, Shi K, Killingsworth CR, Litovsky SH, Powell PC, Kobayashi T, Ferrario CM, Rab A, Aban I, Collawn JF, Dell'Italia LJ (2014) Chymase mediates injury and mitochondrial damage in cardiomyocytes during acute ischemia/reperfusion in the dog. PLoS One 9:e94732. doi:10.1371/journal.pone.0094732 [PubMed: 24733352]
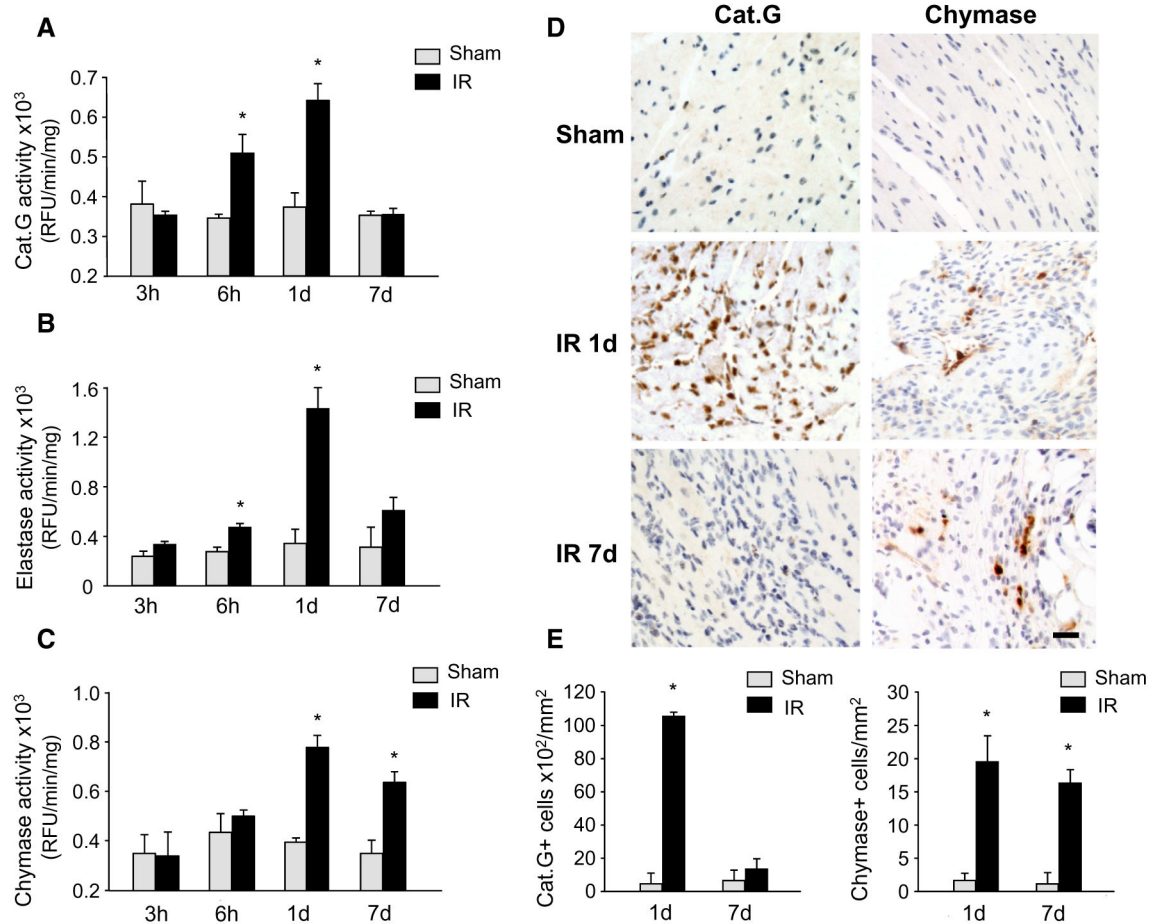
Fig. 1.
Inflammatory serine proteases are elevated after ischemia reperfusion (IR). The left anterior descending artery was ligated for 30 min to induce ischemia and the heart was subsequently reperfused for 3 h, 6 h, 1 or 7 days. Cathepsin G (Cat.G) (**a**), elastase (**b**) and chymase (**c**) activity levels in the hearts of sham and mice subjected to IR injury were assessed by substrate specific enzymatic activity assay. Results are expressed as relative fluorescence units (RFU)/min/mg protein ($n = 6$ for each group). **d** Representative Cat.G and chymase immunostaining of paraffin-embedded heart sections of sham or mice subjected to IR injury. Scale bar: 40 μm. **e** Quantification of Cat.G and chymase-positive cells ($n = 5$ for each group). Values are presented as mean ± SEM, *$P < 0.05$ vs. WT shams
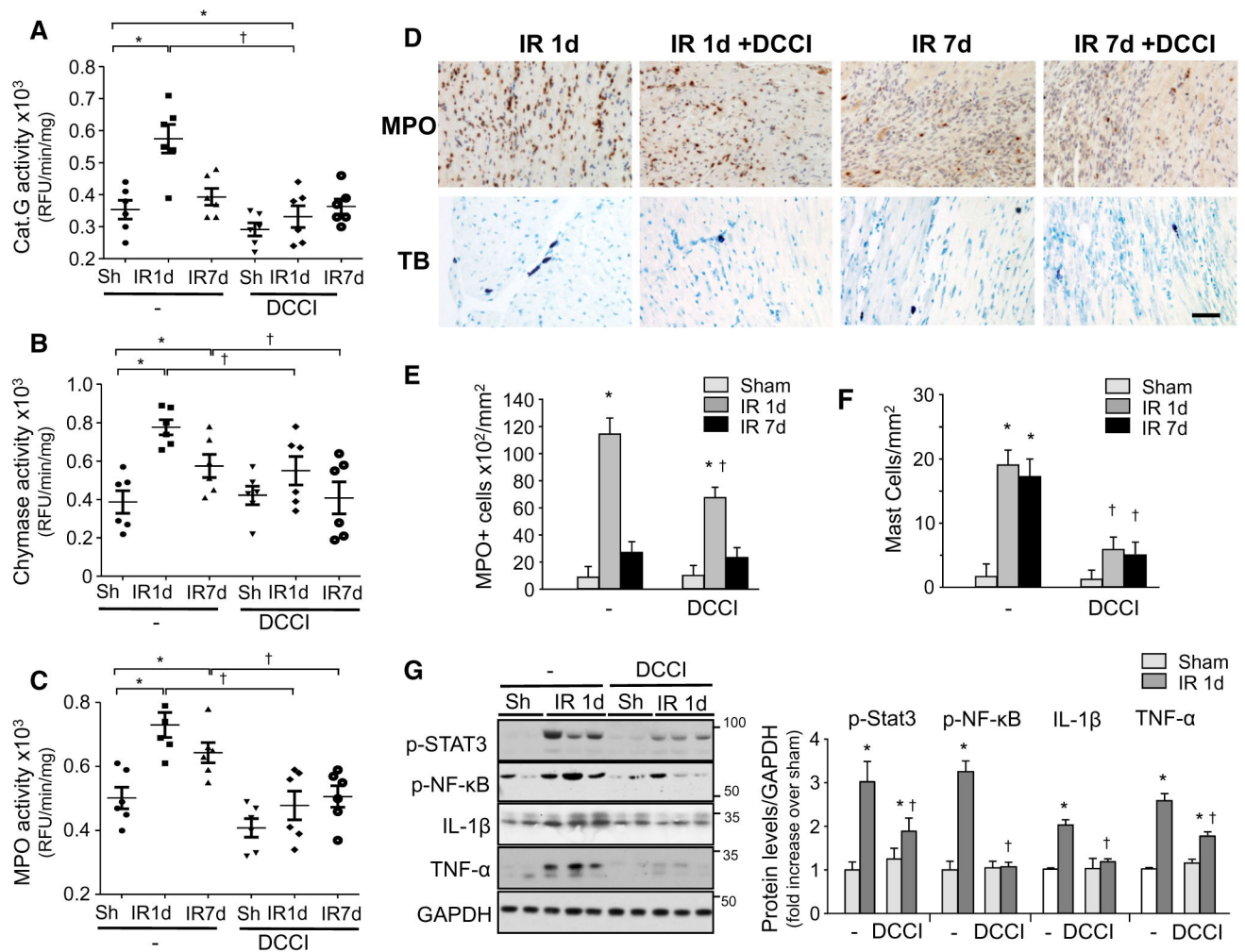
**Fig. 2.**
DCCI treatment attenuates inflammation in the reperfused heart. Cathepsin G (Cat.G) (**a**), chymase (**b**) and myeloperoxidase (MPO) (**c**) activity in the infarcted LV as determined by enzymatic activity assay ($n = 6$ for each group). **d** Representative MPO or toluidine blue (TB) staining of paraffin-embedded heart sections from sham or mice subjected to ischemia reperfusion (IR). Scale bar: 40 μm. **e**, **f** Quantification of MPO- and mast cell-positive cells in mice treated with either vehicle or DCCI ($n = 5$ for each group). **g** Left: immunoblot analysis indicates a decrease in inflammatory signaling in the infarcted region of mice treated with DCCI compared to vehicle post-IR. Right: quantification of experiments represented as fold change compared to sham animals treated with vehicle ($n = 5$ for each group). GAPDH was included as a loading control. Values are presented as mean ± SEM, *$P < 0.05$ vs. shams, †$P < 0.05$ vs. vehicle-treated IR
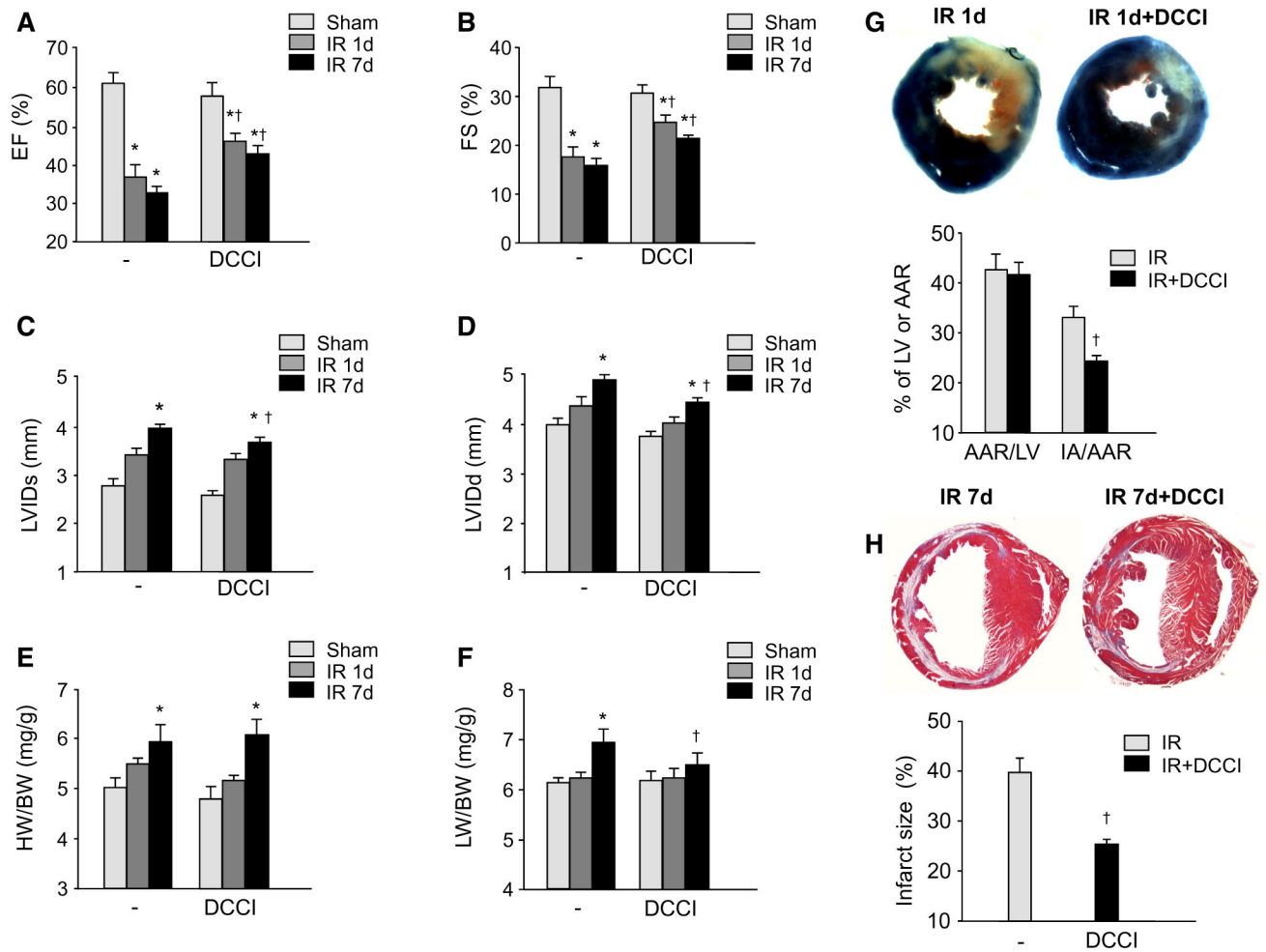
Fig. 3.

DCCI improves cardiac function post-IR. Echocardiography measurement of left ventricular (LV) ejection fraction (EF) (**a**), fractional shortening (FS) (**b**) and LV internal diameter (LVID) in systole (**c**) and diastole (**d**). Effects of DCCI treatment on IR-induced heart weight (HW) (**e**) or lung weight (LW) (**f**) to body weight (BW) ratio ($n = 6$ shams, $n = 8$ IR groups). Top: representative images of Evans blue and diphenyl tetrazolium chloride or Masson's trichrome staining on transverse heart sections at day 1 (**g**) and 7 (**h**) post-IR, respectively. Bottom: quantification of the area at risk (AAR) and infarct area (IA) ($n = 5$ for each group). Values are presented as mean ± SEM, *$P < 0.05$ vs. sham, †$P < 0.05$ vs. vehicle-treated IR
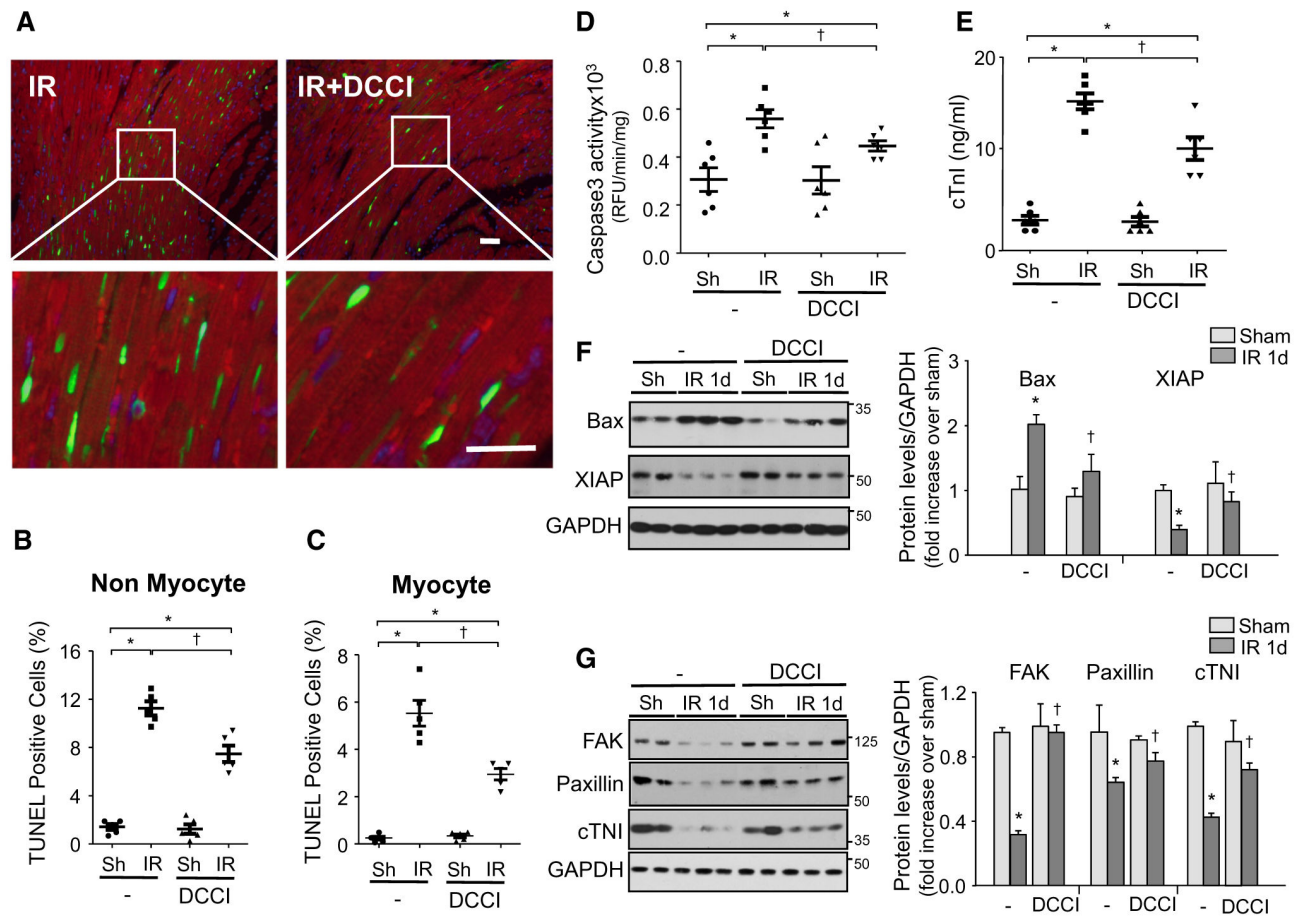
Fig. 4.
DCCI deletion offers cardioprotection after acute IR. Ischemia reperfusion (IR) was induced for 24 h. **a** LV tissue sections were assessed for apoptosis using TUNEL assay (green), tropomyosin (red), and DAPI (4′,6-diamidino-2-phenylindole) (blue) staining. Scale bar: 40 μm. The number of TUNEL-positive myocytes (**b**) and non-myocytes (**c**) in the reperfused area was expressed as a percentage of total nuclei detected by DAPI staining ($n = 5$ each group). **d** Quantification of caspase-3 activity in the LV using caspase-3 specific fluorogenic substrate ($n = 6$ each group). **e** Plasma levels of cardiac troponin-I (cTnI) as determined by ELISA assay in samples from vehicle- or DCCI-treated mice 24 h post-IR ($n = 6$ each group). Immunoblot analysis indicates a decrease in pro-apoptotic signaling (**f**) and focal adhesion signaling (**g**) in the infarcted region of mice treated with DCCI or vehicle post-IR. Left: representative immunoblots. Right: quantification of experiments represented as fold change compared to shams ($n = 6$ each group). GAPDH was included as a loading control. Values are presented as mean ± SEM, $*P < 0.05$ vs. shams, $^{\dagger}P < 0.05$ vs. vehicle-treated
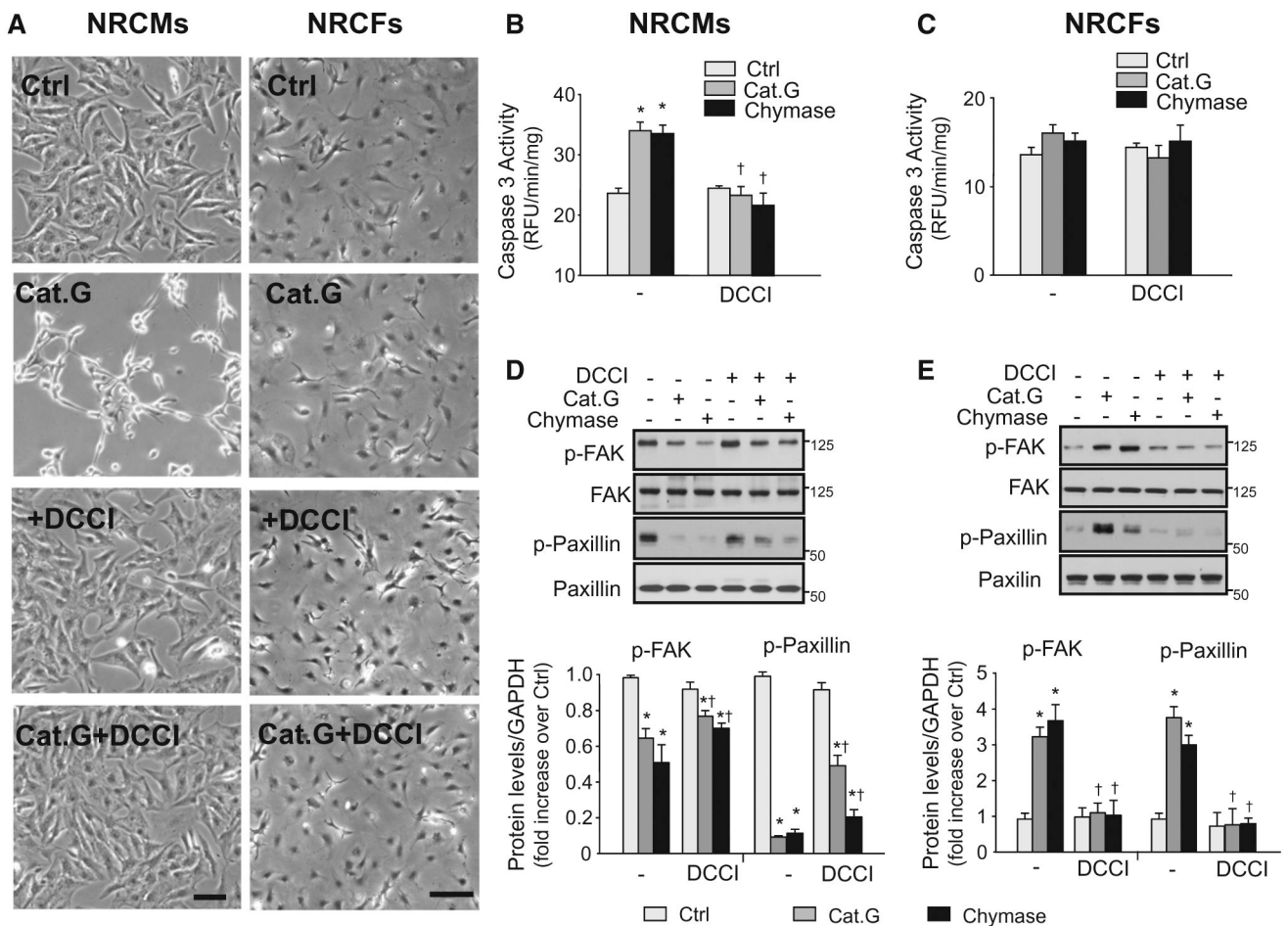
Fig. 5.
Dual effects of cathepsin G and chymase on focal adhesion signaling and cell detachment. Neonatal rat cardiomyocytes (**a**, **b**, **d**) and fibroblasts (**a**, **c**, **e**) were pretreated without or with DCCI (5 μM) prior to treatment with cathepsin G (Cat.G) or chymase for 8 h. **a** Phase-contrast photomicrographs (bar = 100 μm). **b**, **c** Caspase-3 activity was measured using fluorogenic substrate. **d**, **e** Left: representative immunoblots showing focal adhesion (FA) signaling in cardiomyocytes (**d**) and fibroblasts (**f**) treated with Cat.G or chymase for 10 min in the presence of DCCI or its vehicle. Right: quantification of experiments expressed as mean ± SEM from three separate cultures. *$P < 0.05$ vs. control, †$P < 0.05$ vs. vehicle-treated cells
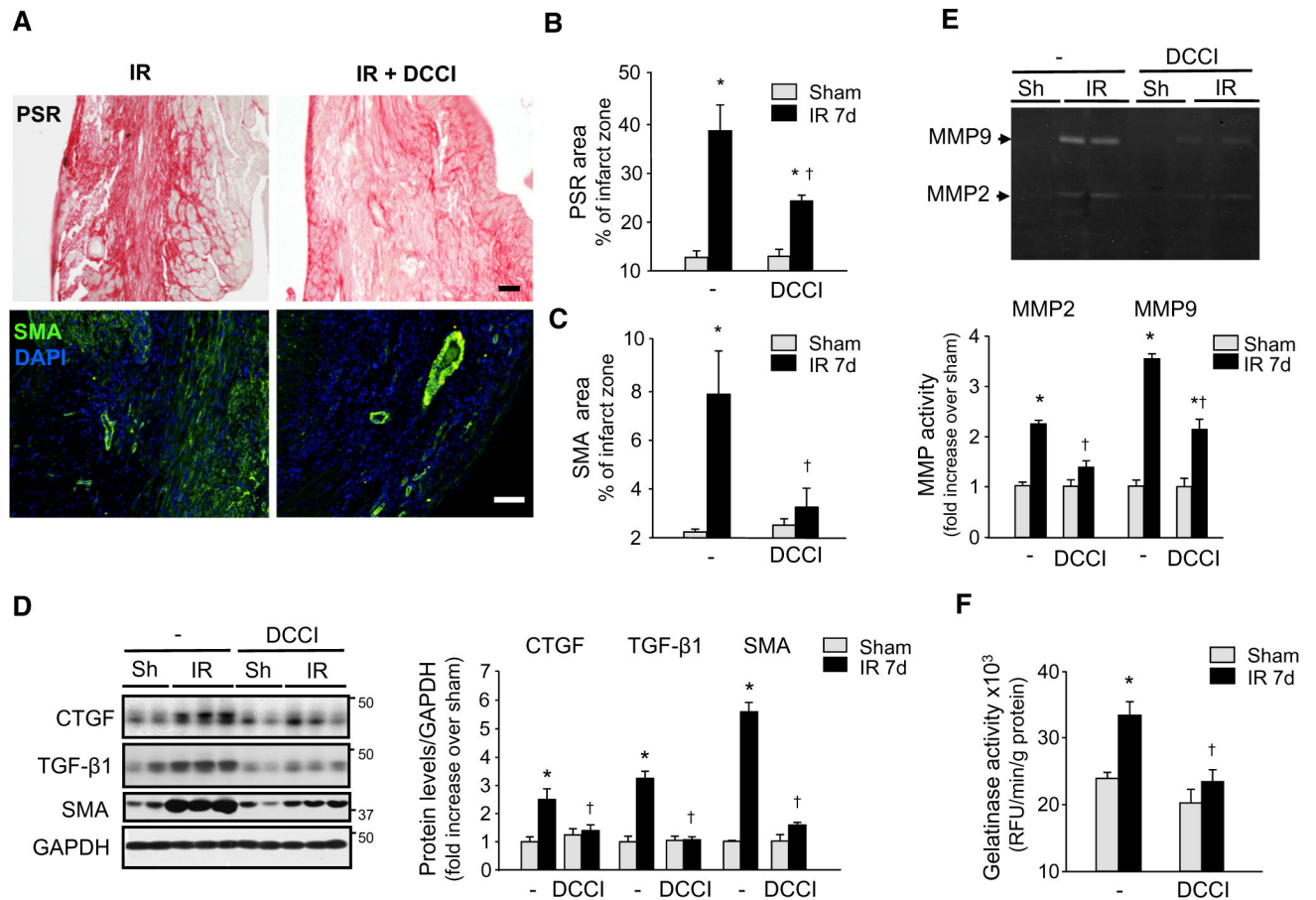
Fig. 6.
DCCI reduces fibrosis and improves cardiac remodeling after IR. Ischemia reperfusion (IR) was induced for 7 days. **a** Picro-sirus red staining and immunohistochemistry against smooth muscle α-actin (SMA) show reduced collagen and myofibroblast deposition in the injured myocardium of mice treated with DCCI compared to those treated with vehicle. Scale bar: 40 μm. Semi-quantitative analysis of collagen staining (**b**) and SMA immunoreactive myofibroblasts (**c**) expressed as a percentage of total infarct area. **d** Immunoblot analysis indicates a decrease in profibrotic signaling molecules in the infarcted region of mice treated with DCCI vs. the treatment with vehicle post-IR. Left: representative immunoblots. Right: quantification of experiments represented as fold change compared to WT animals ($n = 6$ for each group). GAPDH was included as a loading control. e In-gel zymography (top) and relative band density quantification (bottom) indicate a decrease in MMP-2 and −9 activity in the infarcted myocardium of mice treated with DCCI vs. treated with vehicle. **f** Gelatinase activity assay in animals subjected to IR and treated with either vehicle or DCCI ($n = 5$ for each group). Values are presented as mean ± SEM, $*P < 0.05$ vs. shams, $†P < 0.05$ vs. vehicle-treated IR
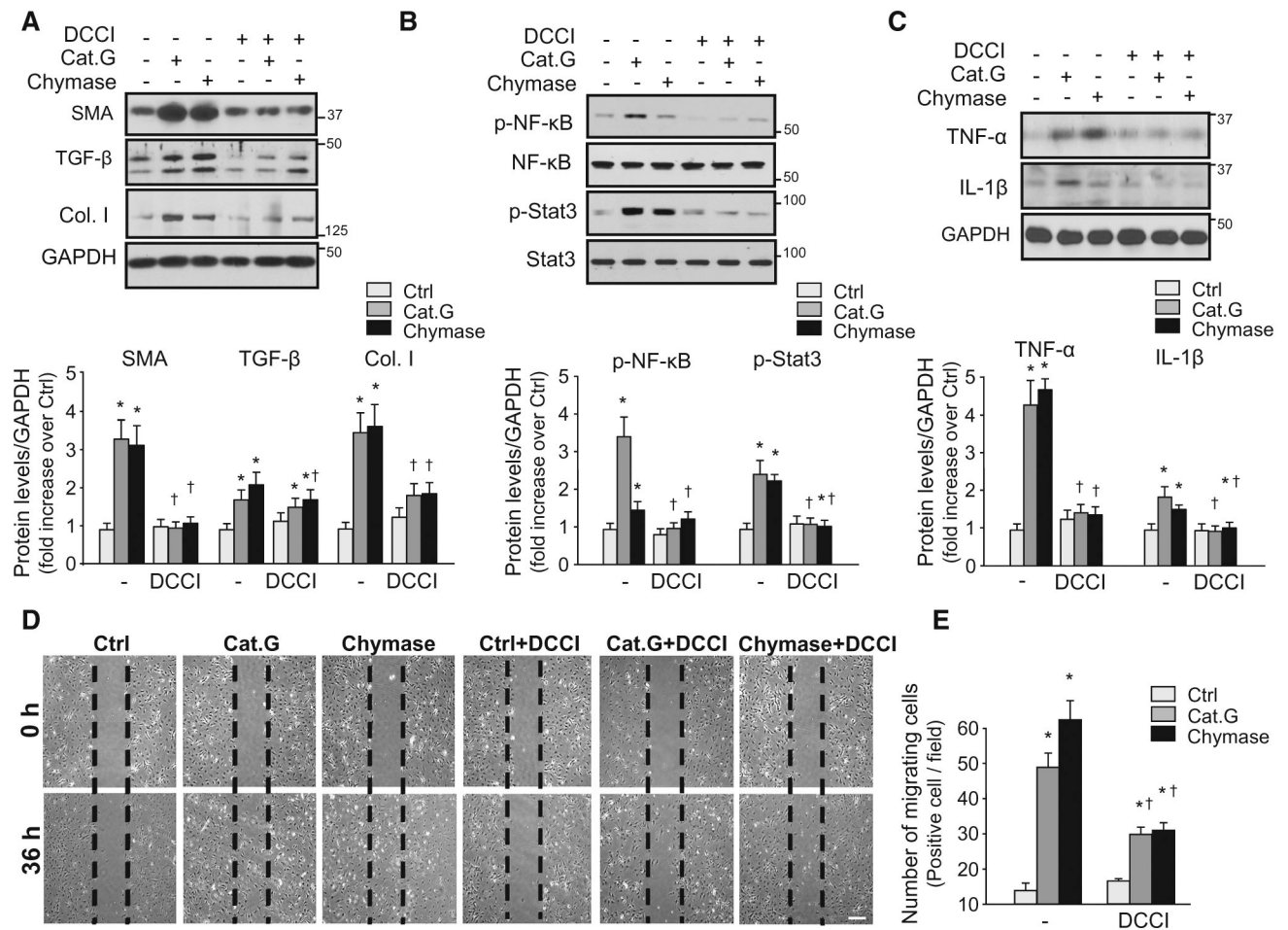
Fig. 7.
Cathepsin G and chymase induce cardiac fibroblast migration and differentiation. **a–c** Neonatal rat cardiac fibroblasts were pretreated with DCCI (5 μM) or vehicle for 15 min and then treated with cathepsin G (Cat.G, 0.02 U/ml) or chymase (100 nM) for 36 h and cell lysates were processed for immunoblot analysis. Top: representative immunoblots. Bottom: quantification of experiments represented as fold change compared to untreated control (Ctrl). GAPDH was included as a loading control. **d** Migration scratch assay was performed to assess the rate of migration of cardiac fibroblasts untreated or treated with Cat.G or chymase with or without DCCI pretreatment. **e** A significant increase in the migration rate was observed in Cat.G- and chymase-treated fibroblasts compared with controls which was attenuated by DCCI treatment. Scale bar: 200 μm. Results are representative of three independent experiments. Data are mean ± SEM; *$P < 0.05$ vs. control; †$P < 0.05$ vs. vehicle-treated fibroblasts